How to cite: *Angew. Chem. Int. Ed.* **2020**, *59*, 22423–22426
International Edition: doi.org/10.1002/anie.202009767
German Edition: doi.org/10.1002/ange.202009767

Structural Biology

Probing Cooperativity of N-Terminal Domain Orientations in the p97 Molecular Machine: Synergy Between NMR Spectroscopy and Cryo-EM

Rui Huang[+], Zev A. Ripstein[+],* John L. Rubinstein,* and Lewis E. Kay**

Abstract: *The hexameric p97 enzyme plays an integral role in cellular homeostasis. Large changes to the orientation of its N-terminal domains (NTDs), corresponding to NTD-down (p97-ADP) or NTD-up (p97-ATP), accompany ATP hydrolysis. The NTDs in a series of p97 disease mutants interconvert rapidly between up and down conformations when p97 is in the ADP-bound state. While the populations of up and down NTDs can be determined from bulk measurements, information about the cooperativity of the transition between conformations is lacking. Here we use cryo-EM to determine populations of the 14 unique up/down NTD states of the homo-hexameric R95G disease-causing p97 ring, showing that NTD orientations do not depend on those of neighboring subunits. In contrast, NMR studies establish that inter-protomer cooperativity is important for regulating the orientation of NTDs in p97 particles comprising mixtures of different subunits, such as wild-type and R95G, emphasizing the synergy between cryo-EM and NMR in establishing how the components of p97 function.*

Protein homeostasis involves coordinated activities of a large number of molecular machines that carry out specific tasks, including protein synthesis and folding, protein disaggregation and refolding, and finally unfolding and subsequent degradation.[1] Elucidating how the components and subunits of the machines involved in these processes work together to perform specific functions is necessary to obtain a detailed understanding of their mechanisms of action. Many of the key molecular players in proteostasis form oligomeric structures, raising the possibility of cooperative interactions between subunits. These complexes include those that are members of the AAA+ (ATPases associated with diverse cellular activities) superfamily.[2–5] In the past several years, building largely on advances in electron cryo-microscopy (cryo-EM), structures of many different AAA+ unfoldases have been obtained, showing that they interact with substrate in a conserved manner.[6–10] Engagement and subsequent unfolding of substrate proceed through formation of a split-ring structure in which protomers of the unfoldase form a helical configuration about the substrate, with the relative positions of subunits on the helix changing in a concerted manner as substrate is processively forced into a central unfoldase pore.[3,6–10] In the case of AAA+ unfoldases the importance of coordinated movement of protomers for function is, thus, clearly established.

p97/VCP in humans (CDC48 in yeast), a member of the AAA+ family, plays a crucial role in many cellular functions, including protein segregation and unfolding.[11–13] Like other unfoldases, it forms a dynamic helical spiral of protomers that unfolds substrate using a coordinated "hand-over-hand" translocation mechanism.[10] Each of the six subunits of the homo-hexameric wild-type (WT) p97 structure is comprised of an N-terminal domain (NTD) and two tandem ATPase domains (D1 and D2) that are organized into two stacked rings in the absence of substrate (Figure 1A). Upon nucleotide hydrolysis, the NTDs of p97 undergo large-scale domain motions from an up conformation in the ATP-bound state, where the NTDs are above the D1 ring, to a down conformation where they are coplanar with D1 in the ADP-loaded conformation (Figure 1A, middle and bottom).[14–16] This nucleotide-state dependent conformational change has been proposed to regulate interactions between p97 and its cofactors.[17–20] Notably, the NTDs make extensive contacts with D1 in the ADP-bound state that stabilize the NTD-down conformation.[17,21,22] Mutations to the NTD–D1 interface, such as R95G (Figure 1A, bottom right), lead to a severe autosomal dominant disorder named multisystem proteinopathy type 1 (MSP1),[23] in which inter-domain interactions are disrupted and the NTD-up/down equilibrium in the ADP-bound state shifted towards the up conformation.[17,18] This perturbation of the up/down equilibrium was previously analyzed by methyl-TROSY based NMR methods.[17,21,22] Notably, the spectral cross-peak positions from residues at the NTD–D1 interface or in the linker connecting the NTD with D1 were shown to follow a linear trajectory for different

[*] Dr. R. Huang,[+] Z. A. Ripstein,[+] Prof. J. L. Rubinstein, Prof. L. E. Kay
Department of Biochemistry, University of Toronto
Toronto, Ontario M5S 1A8 (Canada)
and
Program in Molecular Medicine, Hospital for Sick Children
555 University Avenue, Toronto, Ontario M5G 1X8 (Canada)
E-mail: zevripstein@gmail.com
john.rubinstein@utoronto.ca
kay@pound.med.utoronto.ca
Dr. R. Huang,[+] Prof. L. E. Kay
Department of Molecular Genetics and Chemistry,
University of Toronto, Toronto, Ontario M5S 1A8 (Canada)
Dr. R. Huang[+]
Department of Chemistry, University of Guelph
Guelph, Ontario N1G 1Y4 (Canada)
E-mail: rhuang08@uoguelph.ca
Prof. J. L. Rubinstein
Department of Medical Biophysics, University of Toronto
Toronto, Ontario M5G 1L7 (Canada)
[+] These authors contributed equally to this work.
Supporting information and the ORCID identification number(s) for the author(s) of this article can be found under: https://doi.org/10.1002/anie.202009767.

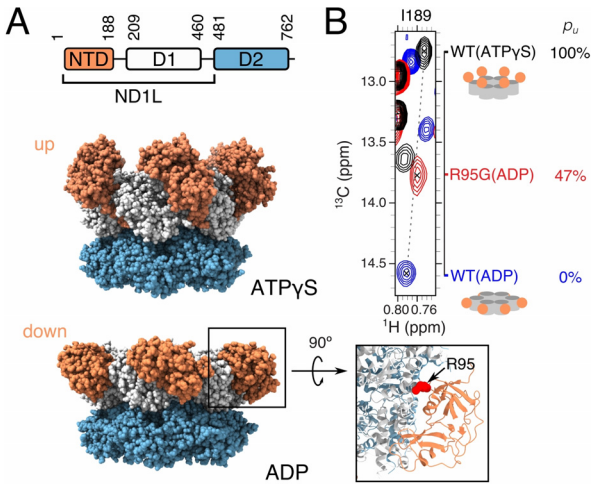

Figure 1. A) (Top) Domain arrangement of full-length and ND1L p97 protomers. (Middle and bottom) Side views of hexameric WT p97 in the ATPγS- (middle, PDB ID 5FTN[14]) and ADP- (bottom, PDB ID 5FTK[14]) bound states. An enlarged cartoon representation (bottom, right) highlights the position of R95, located at the NTD–D1 domain interface. B) Superposition of a selected region from ^{13}C-^{1}H HMQC spectra focusing on the I189δ1 cross-peak (cross-hairs) from WT p97 ND1L in the ADP- (blue) and ATPγS- (black) bound states, as well as from R95G p97 ND1L in the ADP-bound state (red). The fractional population of the NTDs adopting the up conformation (p_u) in the R95G mutant is shown. Data recorded at 18.8 T, 50 °C.

disease mutants extending between chemical shift endpoints derived from WT-ADP (blue) and WT-ATP or ATPγS (black) states (Figure 1 B),[17,21,22] reflecting an up/down equilibrium that is fast on the NMR chemical shift timescale. The relative populations of the interconverting up/down conformers can, therefore, be estimated from the chemical shifts of the methyl probes; for example, in the R95G severe disease mutant, ~47% (p_u) of the NTDs adopt the up conformation, as calculated relative to the 100% up (ATPγS) and 100% down (ADP) reference points (Figure 1 B). The NMR data provide a quantitative measure of the total number of up/down NTDs. However, they do not report on whether the NTD equilibrium is cooperative. For example, is the position of each NTD coupled to the locations of its neighbors, with NTDs collectively exchanging between up/down states much like the synchronous motions of protomers during unfolding of substrates? And if there is cooperativity then how extensive is it?

Here we address these questions using single particle cryo-EM of a homo-hexameric R95G mutant of full-length p97 in the presence of ADP. This mutant was chosen because populations of NTDs in the up and down conformations are approximately equal (Figure 1 B) so that the role of cooperativity can be more easily evaluated than by analysis of mutants with skewed populations. In a previous study, we showed that an initial 3D cryo-EM map could be calculated and refined with C6 symmetry, achieving a resolution of 3.6-Å for the rigid D1 and D2 nucleotide-binding domains of the complex, while the NTD densities were resolved only at low resolution from averaging over 14 different states that reflect the unique combinations of up/down NTD orientations for a hexamer (Figure 2 A).[21] A reference-based 3D classification Scheme[24] revealed multiple species but was not able to reliably quantify populations of different states, as many of

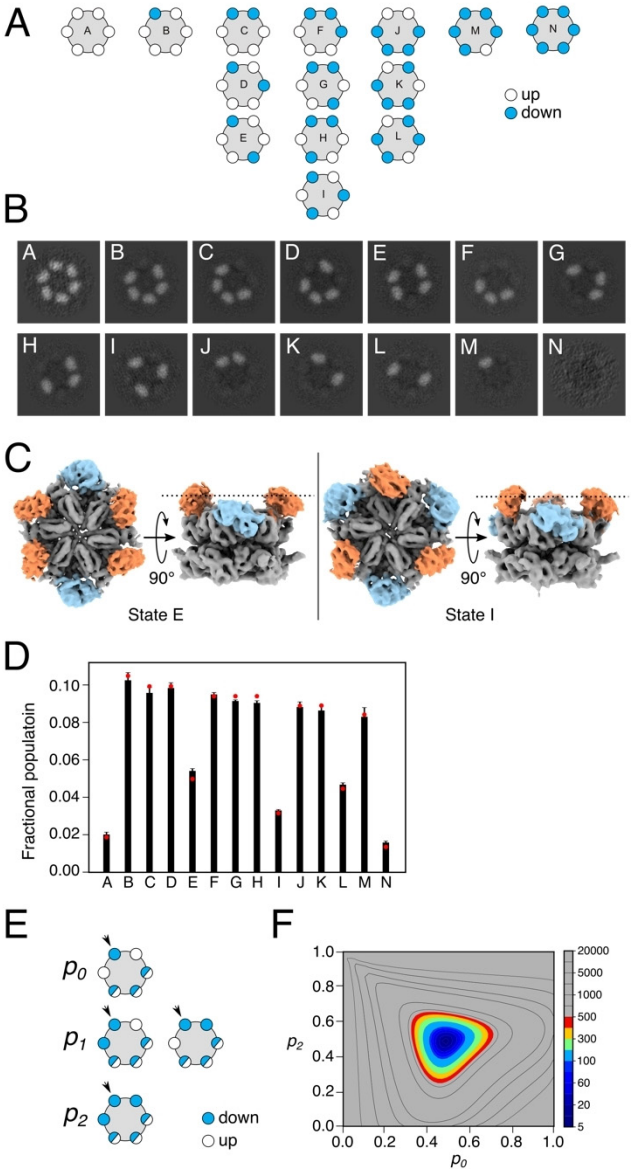

Figure 2. Probing the up/down NTD equilibrium in R95G p97-ADP. A) 14 unique states, corresponding to all possible NTD-up/down configurations in a hexameric p97 structure. B) *z*-slices of 3D reconstructed maps for each of the 14 configurations, with densities originating from the NTD-up conformation. C) Side-views of the reconstructed 3D maps of states E and I, with the position of the *z*-slices in (B) indicated by dashed lines; up and down NTDs are color-coded orange and blue, respectively. D) Fractional populations of the 14 states from analysis of cryo-EM data (black bars) with the standard deviations estimated from four independent datasets (error bars). E) The population distribution in (D) was fitted using a model in which the probability of an NTD (indicated by arrow) orientation depends only on the up or down status of the nearest neighbours. Other subunits are denoted by half-blue/white circles as they are not considered in the model (see the SI). Best-fitted fractional populations are indicated by red dots in (D), corresponding to $p_0 = p_1 = p_2 = 0.49 \pm 0.01$. F) Reduced χ^2 as a function of p_0 and p_2. Note that p_1 is restrained by the values of p_0 and p_2 (see the SI).

the NTDs could not be resolved into well-defined up or down conformations. This likely reflects the large diversity of classes in the dataset, the pseudo-symmetry of the complex, and the skewed fractional populations for some of the 14 states.

In order to quantify the populations of the 14 states, and hence establish whether the movement of each NTD is independent of the position of its neighbours, we have analyzed a cryo-EM map of R95G p97-ADP using a recently available algorithm based on principle component analysis[25] that allows classification of individual NTDs into their up or down configurations. The procedure is described in the SI and in Figure S1. Figure 2B shows z-slices from the reconstructed 3D maps of all 14 configurations, with the position of the slice chosen so as to bisect the NTD densities in the up position, as illustrated in Figure 2C by the dashed lines. Thus, the presence(absence) of density indicates an up(down) NTD conformation. Notably, the patterns of up/down configurations are accurately captured (compare Figures 2A and B), and a total of $51.3 \pm 0.6\,\%$ of the NTDs are classified as being in the up conformation, in good agreement with $p_u = 47\,\%$ obtained from NMR studies (Figure 1B),[21] thus confirming the robustness of the method (also see Figure S2) as well as indicating that neither the cryo-EM cooling procedure nor interactions between the particles and the air–water interface significantly modify the NTD-up/down thermodynamics (see SI).

The fractional populations of each of the 14 states were extracted from our analysis (Figure 2D, black bars, error bars are 1 standard deviation based on an analysis after dividing the dataset into four equal parts; Figure S3) and fit to a model in which an NTD conformation (up or down) depends only on the positions of NTDs from the two immediately neighboring protomers (Figure 2E; SI). In this model, we define the probability of an NTD adopting the down conformation to be p_0, p_1 or p_2 depending on whether 0, 1 or 2 of the adjacent NTDs are in the down position, respectively. Thus, $p_0 = p_1 = p_2$ implies that the up/down equilibrium of an NTD is independent of the status of the neighboring NTDs, corresponding to no cooperativity, while $p_0 < p_1 < p_2$ (neighboring NTDs in the down position increase the probability of a down NTD) and $p_0 > p_1 > p_2$ (a down NTD conformation is favored when the neighboring NTDs are up) indicate positive and negative cooperativity, respectively. A set of equations can be derived, that depend only on p_0, p_1, and p_2, from which the populations of each of the 14 states in Figure 2A are calculated and used to fit the distribution in Figure 2D (red dots correspond to best fit values; see SI for details). It is noteworthy that any two p values restrain the third, so that there are only two fitting parameters. Prior to fitting the cryo-EM population distribution we established that our model predicts distinct profiles for positive, negative, or no cooperativity, so that each of these possibilities can be easily distinguished (Figure S4). Fits of the fractional populations of the 14 states yielded $p_0 = p_2 = 0.49 \pm 0.004$ (Figure 2D&F), from which p_1 was calculated to be 0.49 ± 0.01. Thus, $p_0 = p_1 = p_2$, and the up/down equilibrium for a given NTD in R95G p97-ADP appears not to be influenced by the status of its neighbors.

The above analysis focused on p97-ADP with each protomer containing the R95G disease mutation. However, MSP1 patients are heterozygous with respect to p97 alleles,[23] with one copy each of disease and wild-type (WT) genes, so that their p97 molecules are likely to be heterogeneous in subunit composition.[21,26–28] NMR experiments recorded on p97-ADP in which NMR-active R95G disease protomers are mixed with NMR-silent WT-subunits have shown that the aberrant up/down NTD equilibrium of the disease protomers can be significantly affected by neighboring WT subunits, leading to a partial reversion of the equilibrium towards that of the WT protomer.[21] Thus, taken together, our cryo-EM and NMR data suggest that the extent of the up/down cooperativity depends on the protomer composition of the p97 particle, with little protomer cross-talk in the case of homo-hexameric R95G p97-ADP molecules, but with the potential for considerable interactions between subunits in disease-relevant mixed hexamers. This is especially likely to be the case for severe disease mutants where the intra-protomer NTD–D1 interface is significantly weakened,[17,21,22] increasing the relative influence of neighboring WT subunits. Our work thus highlights the synergy between state-of-the-art cryo-EM and NMR spectroscopy (see SI for a discussion of the synergy between the techniques), emphasizing that the combination of these two technologies provides a unique opportunity to identify the parameters influencing how individual components of a molecular machine work together, such as the NTDs of p97 in this case.

Acknowledgements

Z.A.R. and R.H. were supported by a graduate scholarship (Z.A.R.) and a postdoctoral fellowship (R.H.) from the Canadian Institutes of Health Research (CIHR). L.E.K. and J.L.R. were supported by the Canada Research Chairs program. This research was funded by CIHR grants FDN-503573 (L.E.K.) and PJT-162186 (J.L.R.). Titan Krios cryo-EM data were collected at the Toronto High-Resolution High-Throughput cryo-EM facility supported by the Canadian Foundation for Innovation and the Ontario Research Fund.

Conflict of interest

The authors declare no conflict of interest.

Keywords: cooperativity · electron microscopy · NMR spectroscopy · p97/VCP · protein structures

[1] M. S. Hipp, P. Kasturi, F. U. Hartl, *Nat. Rev. Mol. Cell Biol.* **2019**, *20*, 421–435.
[2] P. I. Hanson, S. W. Whiteheart, *Nat. Rev. Mol. Cell Biol.* **2005**, *6*, 519–529.
[3] C. Puchades, C. R. Sandate, G. C. Lander, *Nat. Rev. Mol. Cell Biol.* **2020**, *21*, 43–58.
[4] J. P. Erzberger, J. M. Berger, *Annu. Rev. Biophys. Biomol. Struct.* **2006**, *35*, 93–114.

[5] J. M. Miller, E. J. Enemark, *Archaea* **2016**, 9294307.
[6] S. N. Gates, A. L. Yokom, J. B. Lin, M. E. Jackrel, A. N. Rizo, N. M. Kendsersky, C. E. Buell, E. A. Sweeny, K. L. Mack, E. Chuang, et al., *Science* **2017**, *357*, 273 – 279.
[7] Z. A. Ripstein, R. Huang, R. Augustyniak, L. E. Kay, J. L. Rubinstein, *eLife* **2017**, *6*, e25754.
[8] C. Puchades, A. J. Rampello, M. Shin, C. J. Giuliano, R. L. Wiseman, S. E. Glynn, G. C. Lander, *Science* **2017**, *358*, eaao0464.
[9] E. A. Goodall, S. N. Gates, G. C. Lander, A. H. De, A. Martin, *Science* **2018**, *362*, eaav0725.
[10] E. Twomey, Z. Ji, T. E. Wales, N. O. Bodnar, S. B. Ficarro, J. A. Marto, J. R. Engen, T. A. Rapoport, *Science* **2019**, *365*, eaax1033.
[11] H. Meyer, M. Bug, S. Bremer, *Nat. Cell Biol.* **2012**, *14*, 117 – 123.
[12] Y. Ye, W. K. Tang, T. Zhang, D. Xia, *Front. Mol. Biosci.* **2017**, *4*, 39.
[13] L. Stach, P. S. Freemont, *Biochem. J.* **2017**, *474*, 2953 – 2976.
[14] S. Banerjee, A. Bartesaghi, A. Merk, P. Rao, S. L. Bulfer, Y. Yan, N. Green, B. Mroczkowski, R. J. Neitz, P. Wipf, et al., *Science* **2016**, *351*, 871 – 875.
[15] J. M. Schuller, F. Beck, P. Lössl, A. J. R. Heck, F. Förster, *FEBS Lett.* **2016**, *590*, 595 – 604.
[16] W. K. Tang, D. Li, C. Li, L. Esser, R. Dai, L. Guo, D. Xia, *EMBO J.* **2010**, *29*, 2217 – 2229.
[17] A. K. Schuetz, L. E. Kay, *eLife* **2016**, *5*, e20143.
[18] S. L. Bulfer, T. F. Chou, M. R. Arkin, *ACS Chem. Biol.* **2016**, *11*, 2112 – 2116.
[19] N. O. Bodnar, T. A. Rapoport, *Cell* **2017**, *169*, 722 – 735.
[20] M. V. Rao, D. R. Williams, S. Cocklin, P. J. Loll, *J. Biol. Chem.* **2017**, *292*, 18392 – 18407.
[21] R. Huang, Z. A. Ripstein, J. L. Rubinstein, L. E. Kay, *Proc. Natl. Acad. Sci. USA* **2019**, *116*, 158 – 167.
[22] A. K. Schütz, E. Rennella, L. E. Kay, *Proc. Natl. Acad. Sci. USA* **2017**, *114*, E6822 – 6829.
[23] G. D. J. Watts, J. Wymer, M. J. Kovach, S. G. Mehta, S. Mumm, D. Darvish, A. Pestronk, M. P. Whyte, V. E. Kimonis, *Nat. Genet.* **2004**, *36*, 377 – 381.
[24] A. Punjani, J. L. Rubinstein, D. J. Fleet, M. A. Brubaker, *Nat. Methods* **2017**, *14*, 290 – 296.
[25] A. Punjani, D. J. Fleet, *bioRxiv* **2020**, https://doi.org/10.1101/2020.04.08.032466.
[26] K. Arhzaouy, K. H. Strucksberg, S. M. Tung, K. Tangavelou, M. Stumpf, J. Faix, R. Schröder, C. S. Clemen, L. Eichinger, *PLoS One* **2012**, *7*, e46879.
[27] C. C. Weihl, S. Dalal, A. Pestronk, P. I. Hanson, *Hum. Mol. Genet.* **2006**, *15*, 189 – 199.
[28] S. Dalal, M. Rosser, D. M. Cyr, P. I. Hanson, *Mol. Biol. Cell* **2004**, *15*, 638 – 648.

Manuscript received: July 15, 2020
Revised manuscript received: August 24, 2020
Accepted manuscript online: August 28, 2020
Version of record online: October 6, 2020

